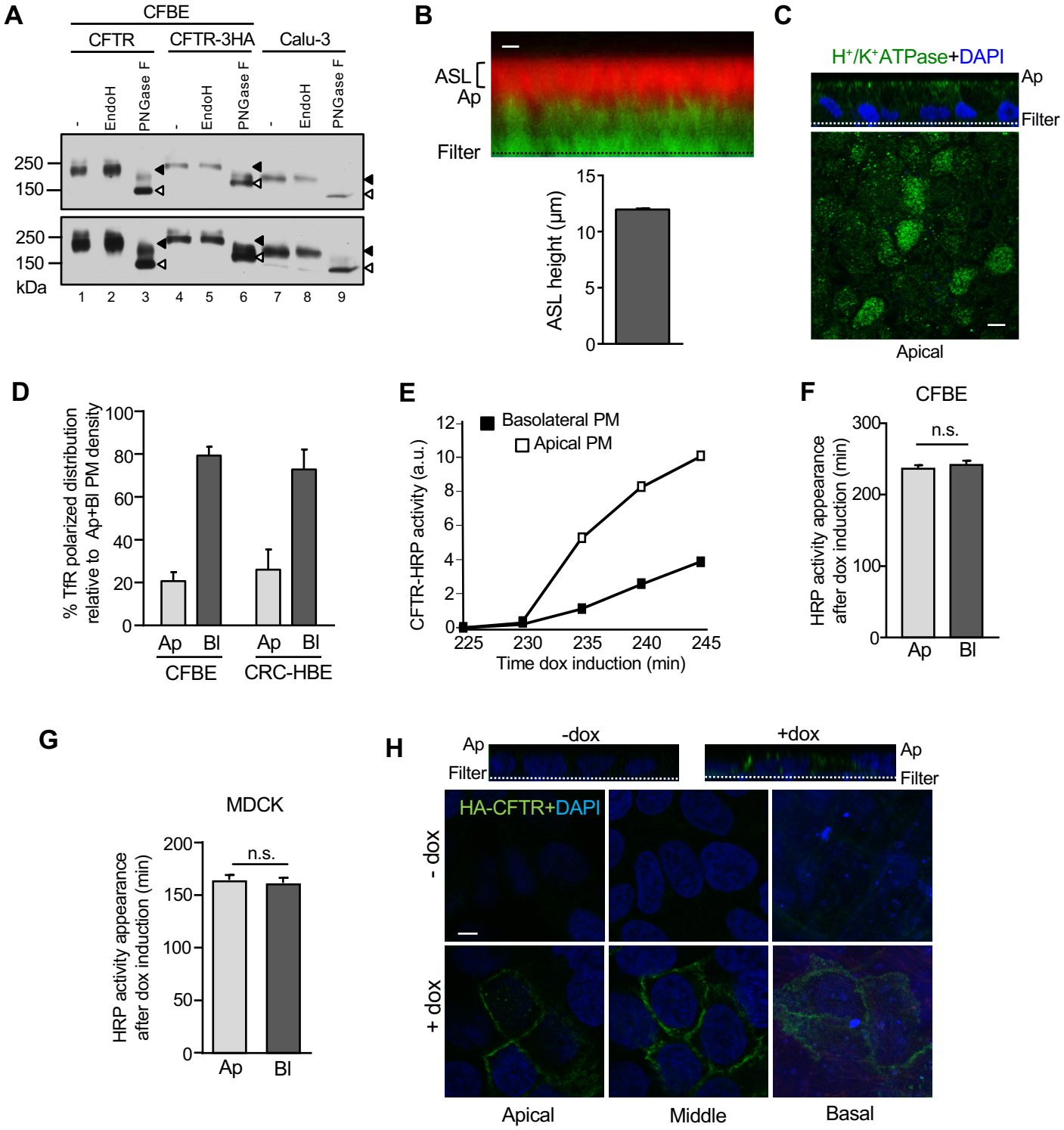

Figure S1. Biochemical and morphological characterization of immortalized (CFBE) and primary conditionally reprogrammed (CR-HBE) human bronchial epithelia.

(A) Electrophoretic mobility shifts of endogenous and exogenous CFTR after endoglycosidase digestion, visualized by immunoblotting. Cell lysates from Calu-3 cells or CFTR and CFTR-3HA expressing polarized CFBE cells were probed with anti-CFTR (L12B4 and M3A7) Abs before or after endoglycosidase H (EndoH) or Peptide-N-Glycosidase F (PNGase F) digestion. Complex-glycosylated and deglycosylated forms of CFTR are indicated by filled and empty arrowheads, respectively.

(B) ALI differentiated CR-HBE and the airway surface liquid (ASL) were stained with Cell tracker (green) and rhodamin-dextran (red), respectively (upper panel). ASL height was determined in 3-10 areas on 2 filters in 2 independent experiments as described in Methods. Bar: 10µm.

(C) Differentiated CR-HBE cells at ALI interface were immunostained for H+/K+-ATPase (green) and the nuclei were visualized with DAPI (blue). Bar: 5µm.

(D) Steady-state PM expression of TfR in filter-grown CFBE and CR-HBE was measured after HRP-Tf loading for 1-3 h at 37° C from the apical or basolateral compartment. HRP activity was measured at both apical and basolateral PM. Surface density is expressed as the % of total PM expression (n=7/CFBE or 4/CR-HBE).

(E-G) Newly synthesized CFTR-HRP concurrently arrives at both PM domains. CFTR-HRP activity was monitored after dox-induction at indicated times in the apical and basolateral compartments. Representative experiment in CFBE is shown in (E) and the mean delay of CFTR-HRP arrival time after dox induction is depicted in CFBE (n=8) and MDCK cells in (G) (n=5).

(H) Specificity of basolateral CFTR staining on filter grown CFBE cells. CFBE were induced (+dox) or not (-dox) in the presence of doxycycline and incubated with anti-HA Ab from the basolateral compartment for 45 min at 37° C, while the apical compartment was supplemented with goat anti-mouse Fab. Indirect immunostaining was done on permeabilized cells and labeled CFTR was visualized by LCFM. Upper panels are representative z-sections. CFTR (green), actin (red) and DAPI (blue). Scale bar, 5µm. Data are means ± SEM on each panel. n.s. non-significant.

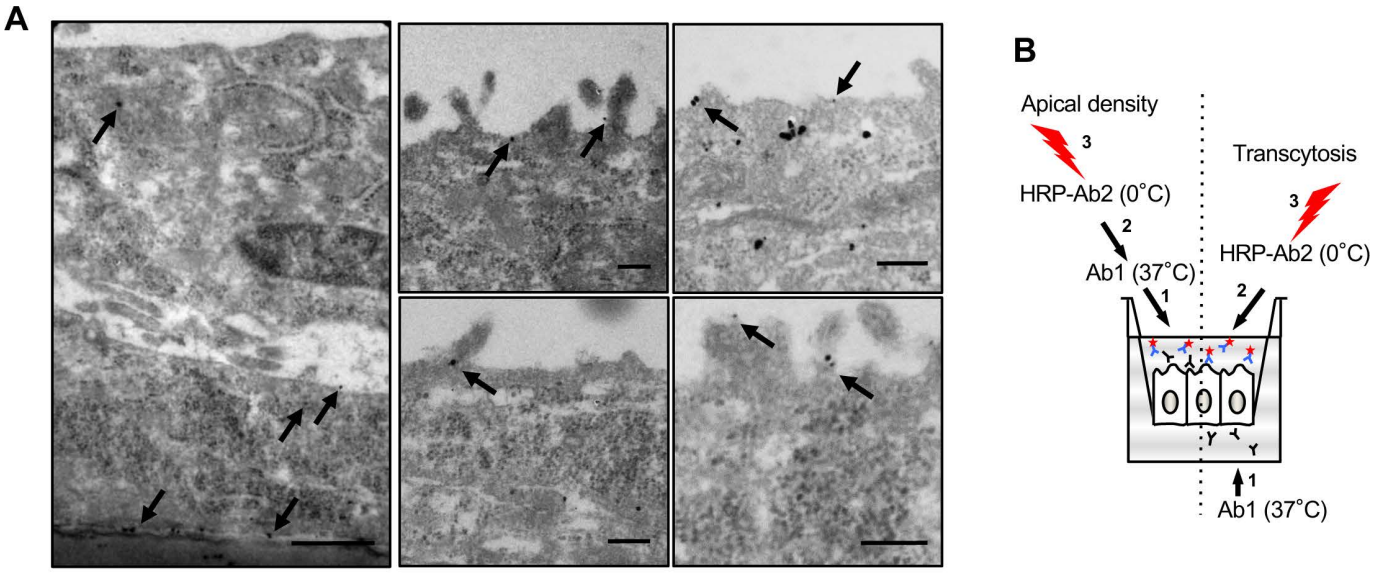

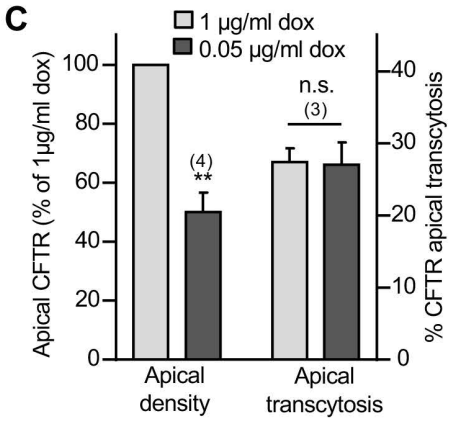

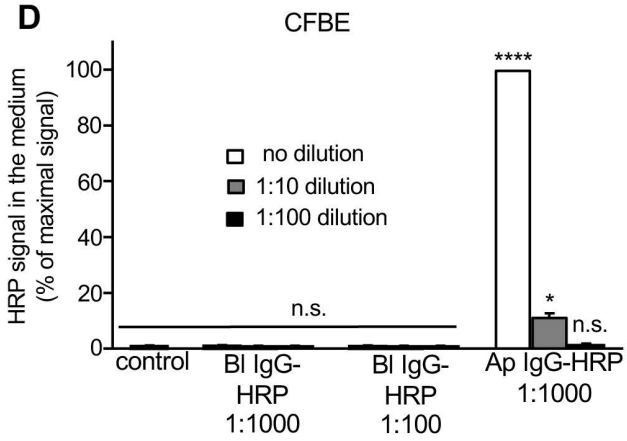

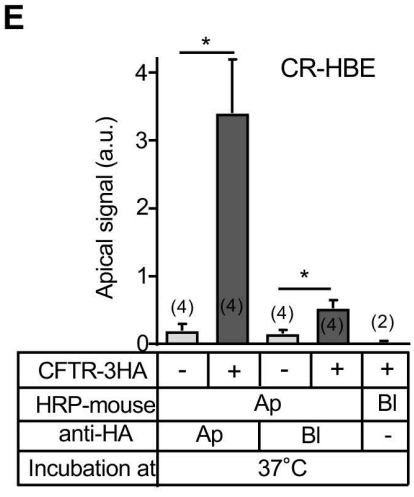

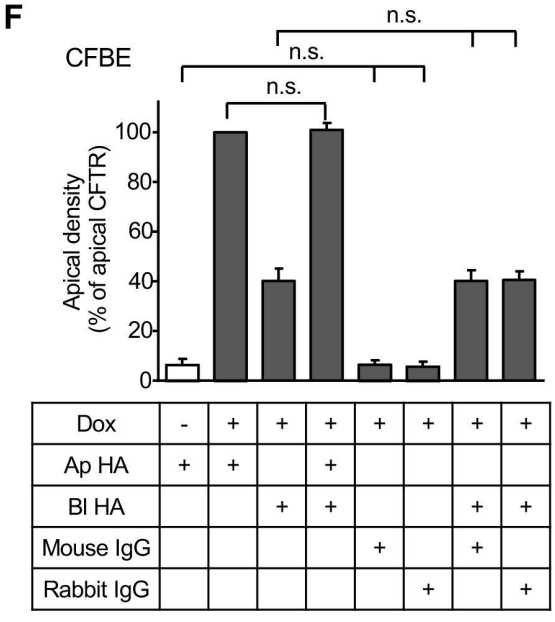

Figure S2. Assay development to monitor CFTR transcytosis in polarized human airway cells.

(A) Immuno-EM detection of CFTR-3HA after basolateral anti-HA labeling (3h, 37°C) in CFBE. CFTR-3HA-anti-HA complexes were revealed with nanogold-conjugated anti-mouse Ab (arrows). Scale bar, 0.2 μm.

(B) Apical transcytosis assay. Basolateral PM proteins were labeled with primary Ab (Ab1) at 37°C (1, right) and the Ab apical appearance was quantified by HRP-conjugated secondary Ab binding (Ab2) in the presence of Amplex Red substrate (2-3, right). In parallel samples, the steady-state CFTR density was determined at the apical PM by PM-ELISA at 37°C (1-3, left).

(C) Relative transcytosis flux of CFTR is unaltered after 50% reduction of the apical CFTR expression. CFTR expression was induced in the presence of 0.05 μg/ml (light gray) or 1 μg/ml (dark grey) doxycycline. At 0.05 μg/ml doxycycline CFTR-3HA expression was ~25% of that detected in Calu-3 cells by quantitative immunoblotting (see also Fig.1A). Apical density and relative transcytosis of CFTR were measured by PM-ELISA.

(D-F) Specificity of the PM-ELISA-based CFTR transcytosis assay in CFBE (D, F) and in CR-HBE (E) cells. (D) HRP-conjugated anti-mouse IgG were incubated in the apical (Ap) or basolateral (Bl) compartment of CFBE cells and HRP activity of diluted apical medium samples was measured in the presence of Amplex Red. Signal was normalized to the maximum HRP activity, obtained with apical IgG-HRP and statistical difference was calculated relative to untreated cells (n=3). HRP-anti-mouse Ab did not traverse the CFBE monolayer to the apical compartment. (E) No significant signal was detected at the apical PM after basolateral (3h, 37° C) incubation of HRP-anti-mouse Ab in CR-HBE. (F) Similar HRP-anti-mouse IgG activity was measured at the Ap PM after Ap or Ap+Bl anti-HA incubation. No significant HRP signal was detectable at the apical PM after basolateral mouse or rabbit IgG alone or in the absence of CFTR expression with anti-HA incubation (n=3).

Data are means ± SEM on each panel, parentheses indicate the number of independent experiments. n.s. non-significant, * $p<0.05$, ** $p<0.01$, **** $p<0.0001$.

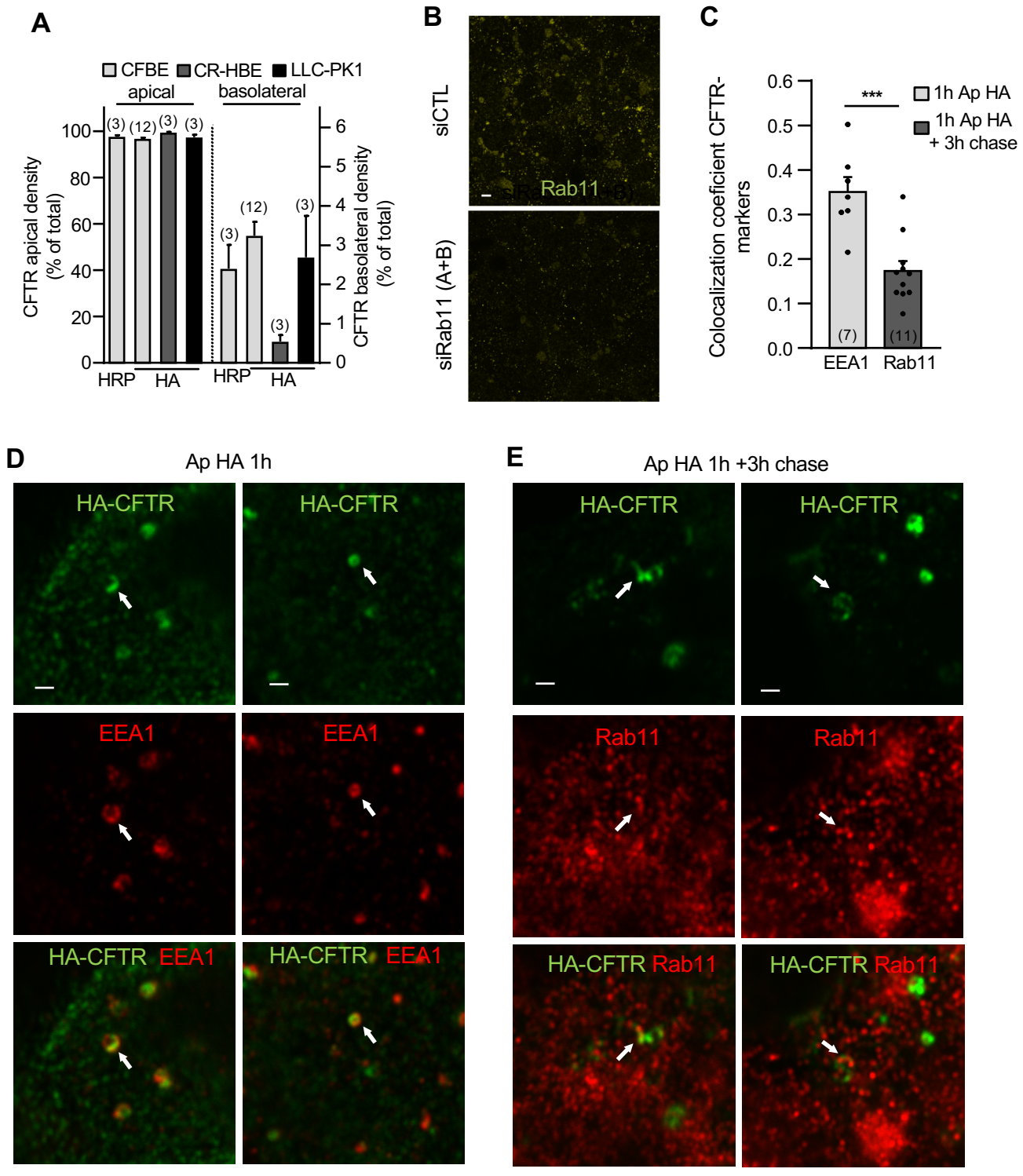

Figure S3. CFTR polarity and trafficking in CFBE cells.

(A) The steady-state apical and basolateral PM density of CFTR-3HA and CFTR-HRP was revealed by PM-ELISA and Amplex Red alone, respectively in CFBE, CR-HBE and LLC-PK1 cells. CFTR domain-specific expression is indicated as percentage of its total PM density.

(B) Specificity of Rab11 immunostaining was confirmed after its ablation with Rab11A+B siRNAs with indirect immunostaining. Scale bar: 5 μm.

(C-E) Apical trafficking of CFTR. CFTR was labelled with anti-HA Abs from the apical compartment (1h, 37°C) in absence or presence of 3h chase at 37°C to accumulate the channel in EEA1+ ASE or Rab11+ ARE, respectively. (C) shows the Mander's colocalization coefficient of apically endocytosed CFTR with organellar markers on whole 3D-volumes (unpaired t-test, ***$p<0.001$) and (D-E) show representative images.

Data are means ± SEM on each panel, parentheses indicate the number of independent experiments (A) or z-stacks (C), ***$p<0.001$.

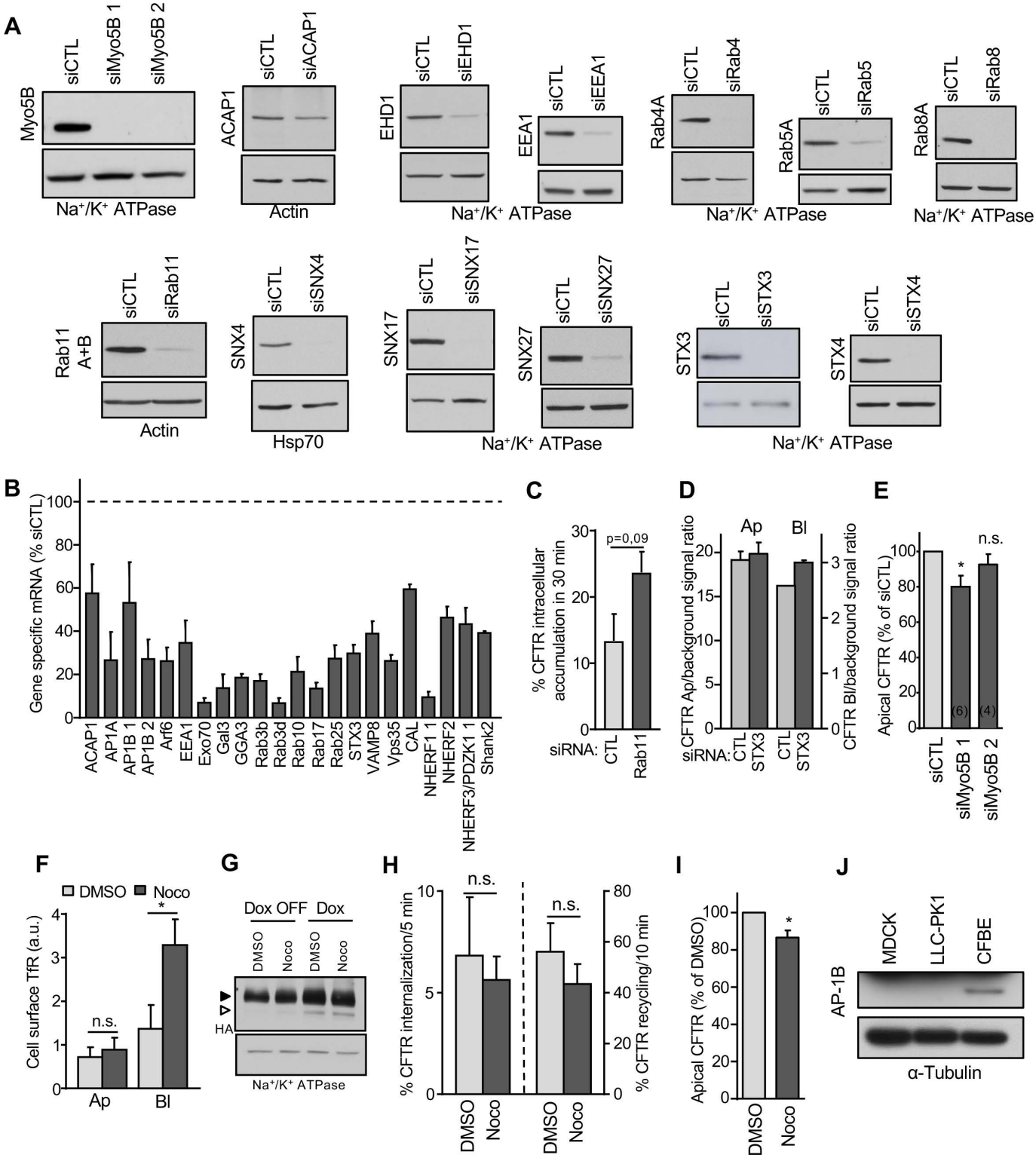

Figure S4. Candidate modulators of CFTR transcytosis.

(A-B) Validation of siRNA mediated silencing of target genes by immunoblotting (A) or qPCR (B) as described in Methods. Na+/K+ ATPase, β-actin and Hsp70 were used as loading controls for the immunoblots. The bar plot includes the means ± SEM of parallel samples from 3-6 independent experiments and expressed as percentage of mRNA expression of siCTL transfected CFBE cells.

(C) Rab11 siRNA leads to an intracellular accumulation of CFTR. Apical CFTR was labelled with anti-HA Ab for 1h on ice and chased (30 min, 37°C) in siRab11 or CTL siRNA transfected CFBE cells (n=5).

(D) STX3 silencing does not compromise the polarity of CFTR. CFTR steady-state PM density was measured by PM-ELISA after 3h anti-HA apical or basolateral labelling at 37°C. Histogram shows the PM signal/PM background (IgG instead of anti-HA Abs) ratio (n=1, 2 technical replicates).

(E) One of the Myo5B siRNA modestly reduces CFTR apical density as compared to that of non-targeted CTL siRNA.

(F) The apical and basolateral PM density of TfR was assayed by PM-ELISA after DMSO (1:1000) or nocodazole (Noco, 33 μM) treatment (3,5h). Ap: apical; Bl: basolateral (n=4).

(G) Inhibition of transcription/translation of CFTR in dox-OFF CFBE cells decreases the core- and complex-glycosylated CFTR, detected by immunoblotting. Nocodazole (33 μM for 3.5 h) has no effect on CFTR expression relative to DMSO. Equal amounts of cell lysates were loaded. Na+/K+-ATPase was the loading control.

(H) MT disruption by nocodazole (Noco, 33μM) does not significantly affect CFTR endocytosis and recycling (n=4). Internalization and recycling were measured by PM-ELISA as described in Methods.

(I) The apical PM density of CFTR was assayed by PM-ELISA after DMSO (1:1000) or nocodazole (Noco, 33 μM) treatment (3,5h) (n=4).

(J) Detection of AP-1B expression by immunoblotting in the indicated cell lines. 30 μg cell lysates were loaded and AP-1B expression was probed. Tubulin was used as loading control.

Data are means ± SEM on each panel, parentheses indicate the number of independent experiments. n.s. non-significant, * $p<0.05$.

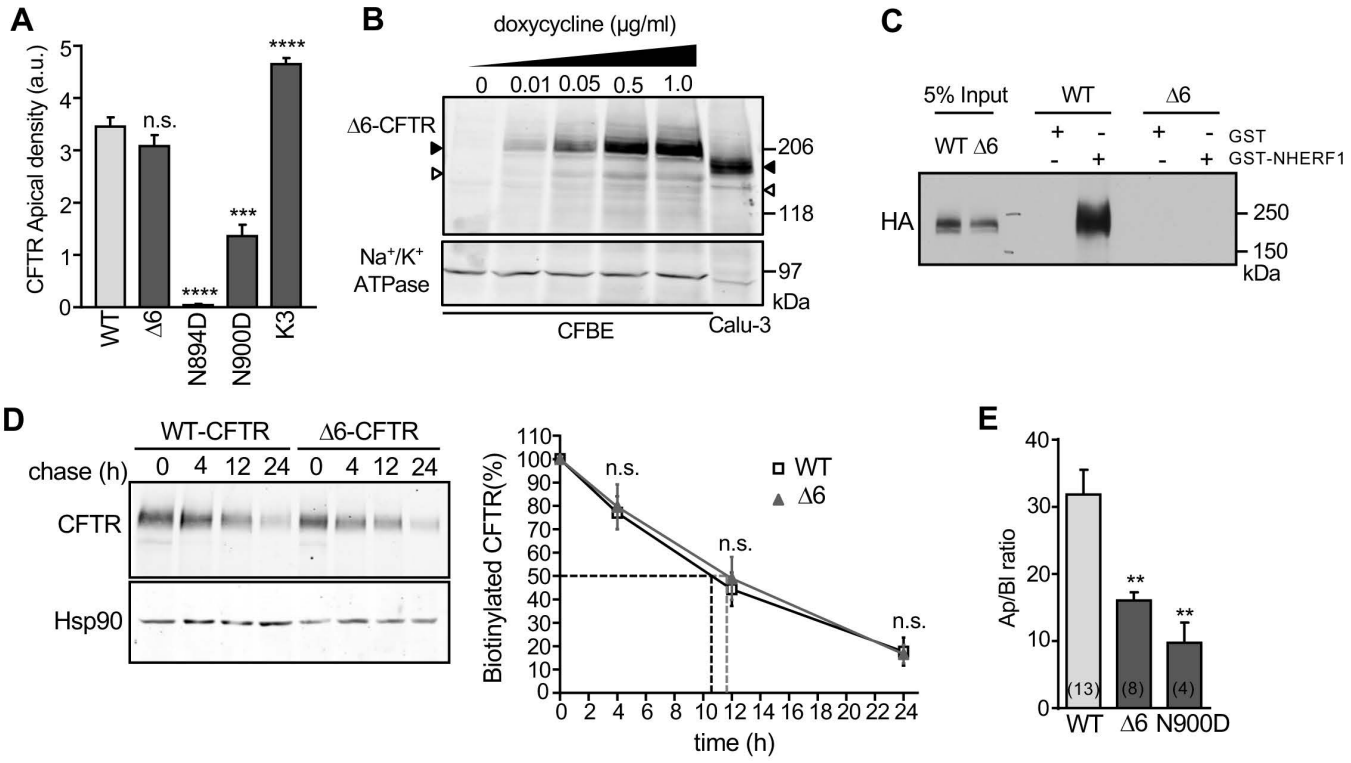

Figure S5. Cellular and biochemical characterization of Δ6-CFTR and other CFTR variants harboring mutant sorting signals.

(A) The effect of putative apical or basolateral sorting signals on CFTR PM expression at the apical domain, measured by PM-ELISA. The abbreviations of the mutations are depicted in Fig. 6A (two-tailed unpaired t-test).

(B) Δ6-CFTR was induced with doxycycline at the indicate concentration for 3 days. CFTR-3HA expression was compared to that of endogenous CFTR of Calu-3 cells in equal amounts of cell lysates by immunoblotting with anti-CFTR Abs. Na+/K+-ATPase was used as loading control.

(C) WT but not Δ6-CFTR binds to recombinant NHERF1. Solubilized WT and Δ6-CFTR were pulled down with recombinant GST- or GST-NHERF1, immobilized on glutathione Sepharose beads. CFTR was probed by immunoblotting together with 5% input of cell lysates with anti-HA Ab and ECL. Representative of 3 independent experiments.

(D) Cell surface stability of WT- and Δ6-CFTR. The PM turnover of CFTR variants was measured by biotinylation with NHS-SS-biotin at 0°C, followed by the indicated chase at 37°C. Biotinylated proteins were immunoprecipitated on monomeric avidin beads and CFTR was visualized by quantitative immunoblotting. Hsp90 was used as loading control. Right panel: quantification of CFTR remaining during the chase (n=3).

(E) WT-, Δ6-, and N900D-CFTR expression ratios at the Ap and Bl (Ap/Bl) PM were measured by comparing the signal obtained at both domains by PM ELISA (parentheses indicate the number of independent experiments, two-tailed unpaired t-test).

(F) NHERF1 siRNA silencing efficiency was monitored by immunoblotting. Na^+/K^+ ATPase was used as loading control.

(G) The blocking efficiency of anti-HA Ab by goat anti-mouse Fab. After anti-HA labeling of CFTR at the apical PM, CFBE cells were incubated on ice with PBSCM (control) or PBSCM-BSA0.5% + goat anti-mouse Fab (1:75). Remaining anti-HA Ab was probed with HRP-conjugated anti-mouse Ab on ice and the specific HRP activity was quantified in the presence of Amplex Red (n=8).

(H) Specificity of NHERF1 detection was confirmed by immunostaining NHERF1 in control (CTL) or NHERF1 1 siRNA transfected CFBE cells. Scale bar: 20µm.

Data are means ± SEM on each panel. n.s. non-significant, ** $p<0.01$, *** $p<0.001$, **** $p<0.0001$.

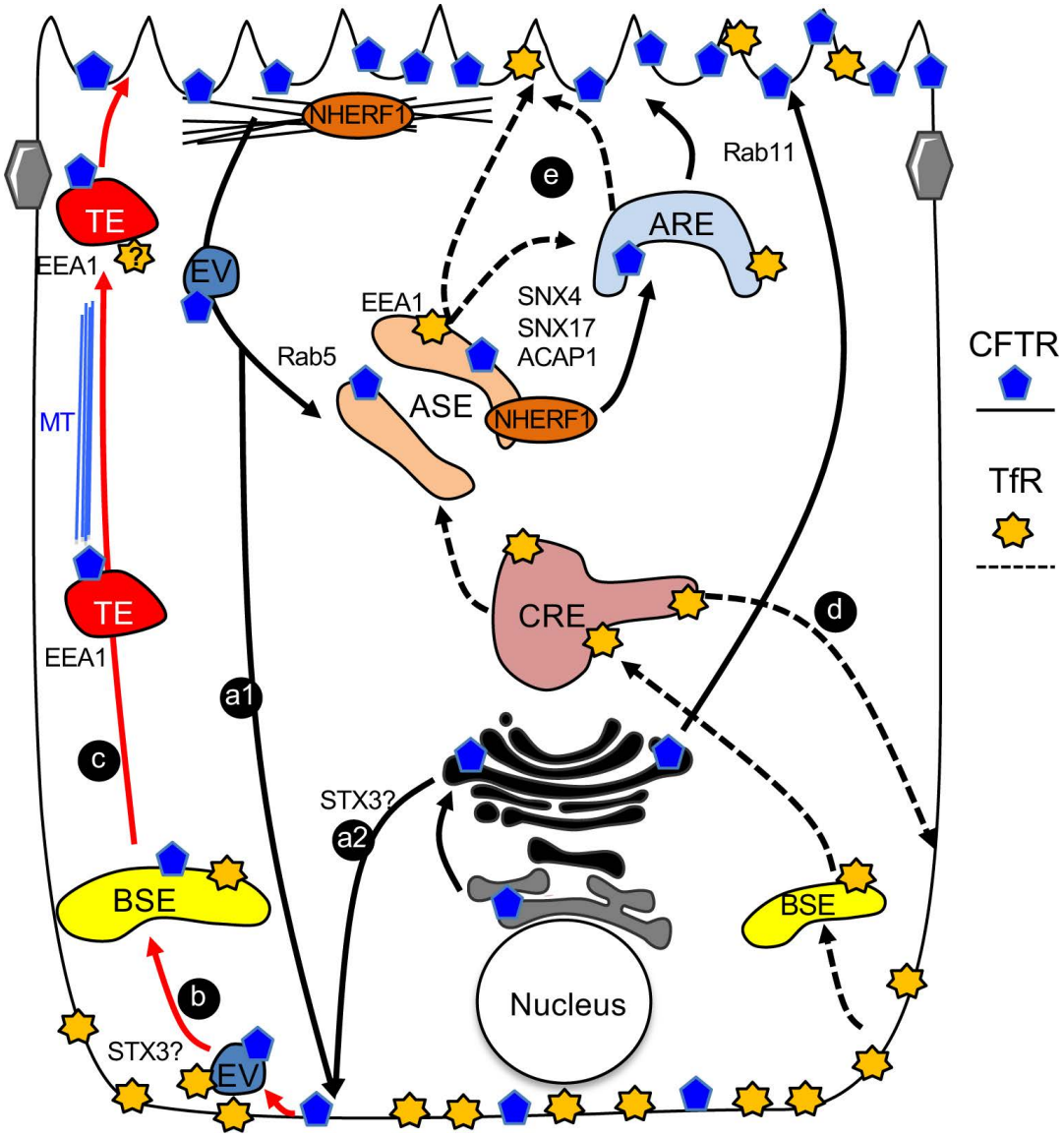

Figure S6. Working model of CFTR transcytosis in airway epithelia.

CFTR basolateral missorting occurs from apical endosomes (a1) and at the TGN along the biosynthetic pathway (a2). (b) Missorted basolateral CFTR is retrieved from the basolateral PM into basolateral sorting endosomes (BSE). (c) CFTR is packaged into EEA1 positive transcytotic endosomes (TE) from BSE and ferried to the apical pole in a microtubules-dependent pathway. (d) The basolateral internalization, recycling and (e) transcytotic route of TfR is indicated by dashed lines for comparison (Perez Bay et al., 2013). While in AP1B-KD MDCK cells transcytotic TfR traverses the ARE, in CFBE cells the ARE may have a minor role in TfR delivery to the apical PM. ASE, Apical Sorting Endosome; ARE, Apical Recycling Endosome; BSE: Basolateral Sorting Endosome; CRE: Common Recycling Endosome; EV, Endocytic Vesicles; Bundled blue lines, microtubules (MT); interlaced black lines: cortical F-actin.

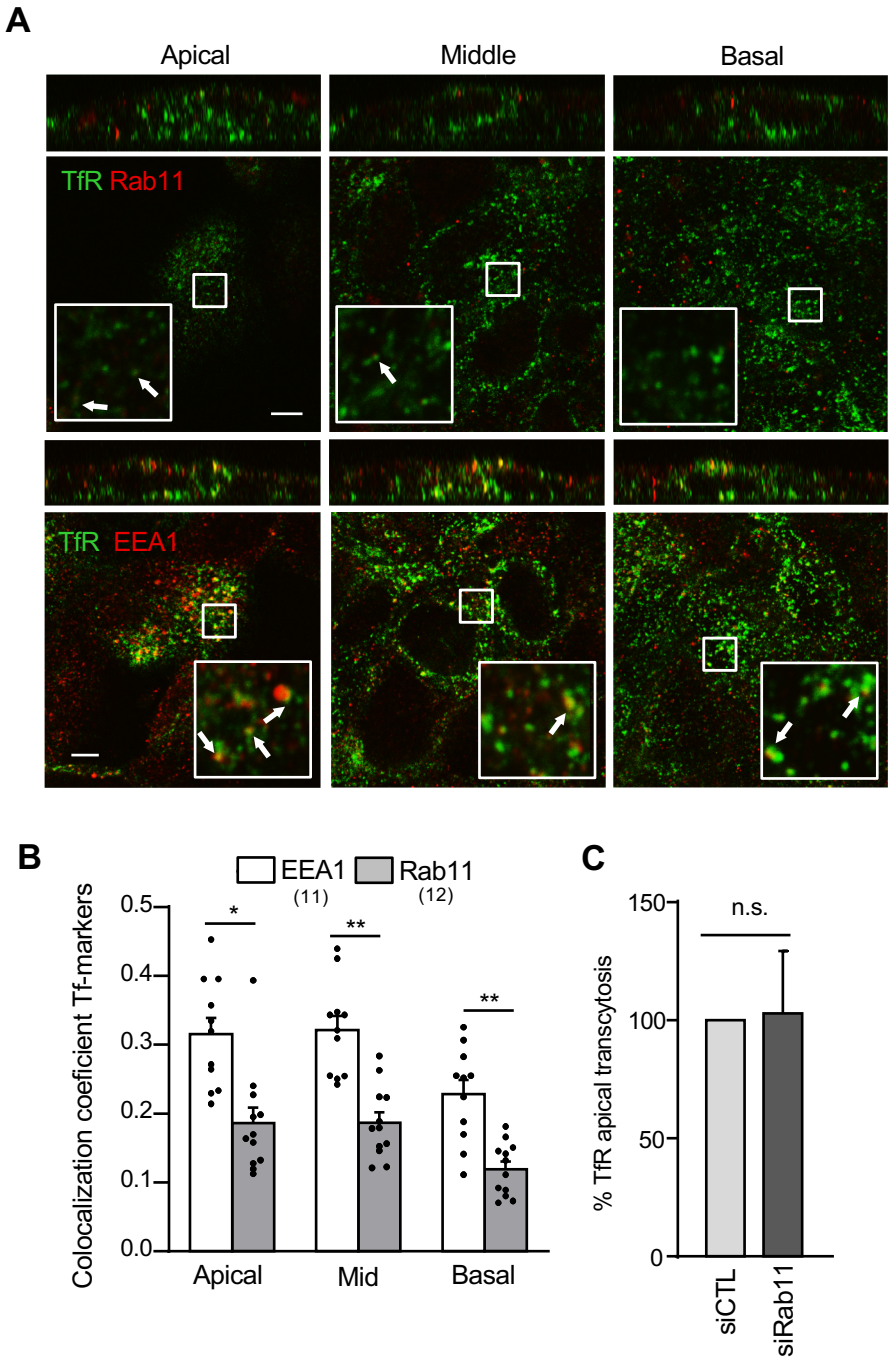

Figure S7. Characterization of TfR transcytotic pathway in CFBE.

(A-B) Transcytotic TfR colocalization with CFTR, EEA1 and Rab11. (A) After endogenous Tf depletion (1h, serum-free medium), Tf-Cy3 was loaded for 45min-1h at 37°C in serum-free medium (green), then cells were fixed and co-stained for EEA1 or Rab11 (red). Inserts are selected areas at ~3.5-fold increased magnification. (B) Quantitative colocalization of transcytotic TfR with EEA1 and Rab11 was measured by the Mander's coefficient on each slice of 3D-volumes (parentheses indicate the number of z-stacks from 2 independent experiments) that were sorted in 3 sections (apical, middle and basal), two-tailed unpaired t-test.

(C) TfR apical transcytosis was measured after 3h of Tf-HRP uptake from the basolateral compartment in CFBE cells transfected with control (CTL) or Rab11A+B siRNAs (n=3). Scale bar: 5 µm.

Data are means ± SEM on each panel. n.s., non-significant, *p<0.05, **p<0.01.

Table S1. Antibodies used in this study. IF, Immunofluorescence; WB, immunoblotting

Name	Host	Reference -Company	Dilution
Monoclonal anti-ACAP1 (B-11)	mouse	sc-376574 -Santa Cruz	1 :100/WB
Monoclonal anti-acetylated-tubulin (6-11B-1)	mouse	T7451 -Sigma	1 :100/IF
Monoclonal anti-beta-actin (mAbcam 8226)	mouse	ab8226 -AbCam	1 :300/WB
Polyclonal anti-AP1M2	rabbit	bs-13638R -Bioss	1 :1000/WB
Monoclonal anti-CFTR (L12B4)	mouse	MAB3484 -Millipore	1 :1000/WB
Monoclonal anti-CFTR (M3A7)	mouse	MAB3480 -Millipore	1 :1000/WB
Monoclonal anti-EBP50/NHERF1 (clone6)	mouse	611160-BD -Trans lab	1 :1000/WB
Monoclonal anti-EGFR (ICR10)	rat	GTX20231 -GeneTex	1 :2000/ELISA
Monoclonal anti-H+K+ ATPase (2G11)	mouse	ab2866 -AbCam	1 :200/IF
Monoclonal anti-HA.11 (16B12)	mouse	MMS-101R -Covance	1 :2000/WB
Monoclonal anti-Hsp70/Hsc70/Hsp73 (1B5)	rat	ADI-SPA-815-D -Enzo	1 :1000/WB
Monoclonal anti-Hsp90 (K41009)	rat	ADI-SPA-839-050 -Enzo	1 :1000/WB
Monoclonal anti-mucin5A/C (45M1)	mouse	MS-145-P0 -ThermoFisher	1 :200/IF
Monoclonal anti-Na+K+ ATPase (H-3)	mouse	sc-48345 -SantaCruz	1 :5000/WB
Monoclonal anti-SNX27 (1C6)	mouse	ab77799 -AbCam	1 :500/WB
Monoclonal anti-SNX4 (B-4)	mouse	sc-271147 -SantaCruz	1 :300/WB
Monoclonal anti-syntaxin4 (49)	mouse	610439 -BD Biosciences	1 :500/WB
Polyclonal anti-EBP50/NHERF1	rabbit	ab3452 -AbCam	1 :200/IF
Polyclonal anti-EEA1	rabbit	PA1-063A -ThermoFisher	1 :300/IF
Monoclonal anti-EHD1	rabbit	EPR4954 -AbCam	1 :2000/WB
Polyclonal anti-myosin5B	rabbit	PAB23710 -AbNova	1 :1000/WB
Polyclonal anti-Rab11	rabbit	R5903 -Sigma	1 :500/IF, 1 :1000/WB
Polyclonal anti-Rab4 (EPR3042)	rabbit	GTX62731 -GeneTex	1 :500/WB
Polyclonal anti-Rab5 (S-19)	rabbit	sc-309 -SantaCruz	1 :1000/WB
Polyclonal anti-Rab8A	rabbit	55296-1-AP -ProteinTech	1 :200/IF, 1:300/WB
Polyclonal anti-SNX17	rabbit	10275-1-AP -ProteinTech	1 :300/WB
Polyclonal anti-syntaxin 3 (H-33)	rabbit	sc-135259 -SantaCruz	1 :200/WB
Monoclonal anti α-tubulin (DM1A)	mouse	T9026 -Sigma	1 :5000/WB
Polyclonal anti-ZO-1 (mid)	rabbit	40-2200 -Invitrogen	1 :100/IF

Table S2. siRNAs used in this study. Bold siRNAs are stealth RNAi obtained from Invitrogen. All other predesigned siRNAs were obtained from Qiagen/Origene.

Gene	Product name
CTL	**Control stealth Med GC**
NHERF1 1	**HSS145123**
NHERF1 2	Hs_SLC9A3R1_5
NHERF2	**HSS113866 ; HSS113867**
PDZK1 1	Hs_PDZK1_8
PDZK1 2	**HSS107800 ; HSS182218**
Shank2 1	**HSS117944 ; HSS177049**
Shank2 2	Hs_SHANK2_9 ; Hs_SHANK2_10
CAL	**HSS126013**
NHERF4	**HSS188224**
Rab3b	Hs_RAB3B_3 ; Hs_RAB3B_4
Rab3d	Hs_RAB3D_3 ; Hs_RAB3D_4
Rab4	Hs_RAB4A_5 ; Hs_RAB4A_6
Rab5	Hs_RAB5A_5 ; Hs_RAB5A_8
Rab8	Hs_RAB8A_4 ; Hs_RAB8A_5
Rab10	Hs_RAB10_3 ; Hs_RAB10_5
Rab11	Hs_RAB11A_5 ; Hs_RAB11A_6 ; Hs_RAB11B_1 ; Hs_RAB11B_6
Rab17	Hs_RAB17_4 ; Hs_RAB17_5
EEA1	Hs_EEA1_5 ; Hs_EEA1_7 ; Hs_EEA1_9
Rab25	Hs_RAB25_1 ; Hs_RAB25_3
EHD1	Hs_EHD1_3
Vps35	Hs_VPS35_5 ; Hs_VPS35_6 ; Hs_VPS35_8
ACAP1	Hs_CENTB1_1 ; Hs_CENTB1_5
Arf6	Hs_ARF6_5 ; Hs_ARF6_8
GGA3	Hs_GGA3_1 ; Hs_GGA3_9
SNX4	Hs_SNX4_2 ; Hs_SNX4_7
SNX17	Hs_SNX17_1 ; Hs_SNX17_2
SNX27	Hs_SNX27_5 ; Hs_SNX27_6
STX3	SR321926-A
STX4	Hs_STX4A_2 ; Hs_STX4_1
Vamp8	**HSS189495**
Exo70	Hs_EXOC7_5 ; Hs_EXOC7_6
Gal3	Hs_LGALS3_7 ; Hs_LGALS3_3 ; Hs_LGALS3_8
AP1A	Hs_AP1M1_1 ; Hs_AP1M1_6
AP1B 1	Hs_AP1M2_5 ; Hs_AP1M2_6 ; Hs_AP1M2_8
AB1B 2	Hs_AP1M2_7 ; Hs_AP1M2_9 ; Hs_AP1M2_10
Myo5B 1	**HSS181415**
Myo5B 2	Hs_MYO5B_7 ; Hs_MYO5B_10

Table S3. qPCR primers used in this study

Gene symbol	Direction	Sequence
CFTR	forward	AGTGGAGGAAAGCCTTTGGAGT
	reverse	ACAGATCTGAGCCCAACCTCA
GAPDH	forward	CATGAGAAGTATGACAACAGCCT
	reverse	AGTCCTTCCACGATACCAAAGT
ACAP1	forward	CTGAGATGACGGTCAAGCTG
	reverse	AGACCAGTGCCCAGTTTCAG
AP1A (AP1M1)	forward	GAGGTGTTCTTGGACGTCATC
	reverse	CATGCCCGAGAGGAAGACT
AP1B (AP1M2)	forward	GGCCAGGTCCACTTCCTATG
	reverse	GCAACTCGTAGACGATGACAAA
ARF6	forward	AGGAACTGGTATGTGCAGCC
	reverse	GATTTCTCTCCTTCCAGGGG
EEA1	forward	ACCCCGAGTAGTGAGTGGC
	reverse	CTTGAGAGCCAACTCTCCCA
EXO70 (EXOC7)	forward	TTCCTCTGGGGTTCCCTACT
	reverse	ACGCAGTGGATGTAGGCAT
GAL3 (LGALS3)	forward	CTGGGGAAGGGAAGAAAGAC
	reverse	CCCGATGATTGTACTGCAAC
GGA3	forward	AAGGGGAAAGCCTGGAGTC
	reverse	CCTTCCAGCTCCTTGTTGAT
RAB3B	forward	GTGGGCATCGACTTCAAGGT
	reverse	CCCACGGTAATAGGCTGTTG
RAB3D	forward	GTGGGGAACAAGTGTGACCT
	reverse	CATTGATGTTCTCCTTGGCA
RAB10	forward	CCTTTTTCGTTTTTCGGATG
	reverse	GGCCTGCTGTATCCCATATC
RAB17	forward	AGCTGGTTCTCCTGGGAAGT
	reverse	ACCACCTTTGTGAAGAACGC
RAB25	forward	CAAGATGGGGAATGGAACTG
	reverse	CTGTCGTGGCTGAACTCATT
STX3	forward	TCGGCAGACCTTCGGATTC
	reverse	TCCTCATCGGTTGTCTTTTTGC
VAMP8	forward	TTATGACCCAGAATGTGGAGC
	reverse	CTTCTGCGATGTCGTCTTGA
VPS35	forward	TTTTGGAGCTGGTGGAAATC
	reverse	TCTGGCATTTCTTTTCCCAT
CAL	forward	AGAAGATGACCAGCCTGAGC
	reverse	CTCTGCTTGGGTTTCTGTCA
NHERF1/EBP50	forward	GGGGCTGGCAACGAAAATG
	reverse	GACCGGATGAACTGGCCTG
NHERF2/E3KARP	forward	CTGGTTCCGACAAGGACACTG
	reverse	CAGGAAGGGGCTCAGAAGTT
NHERF3/PDZK1	forward	GTGTAGCCCAGCAGAGAAG
	reverse	ACCAGATCCACAACCTGCAT
SHANK2	forward	GACTAAGGACCGGGGACTTC
	reverse	TGACCACCTTAAGGACCAGG